Synthesis and magnetic properties of $Fe_{100-x}Mo_x$ alloy nanowire arrays*

Gao Hua(高 华), Gao Da-Qiang(高大强)†, and Xue De-Sheng(薛德胜)

Key Laboratory for Magnetism and Magnetic Materials of the Ministry of Education, Lanzhou University, Lanzhou 730000, *China*

(Received 9 September 2010; revised manuscript received 25 January 2011)

The $Fe_{100-x}Mo_x$ ($13 \leq x \leq 25$) alloy nanowire arrays are synthesized by electrodeposition of $Fe^{2+}$and Mo^{2+} with different ionic ratios into the anodic aluminum oxide templates. The crystals of $Fe_{100-x}Mo_x$ alloy nanowires gradually change from polycrystalline phase to amorphous phase with the increase of the Mo content and the nanowires are of amorphous structure when the Mo content reaches 25 at%, which are revealed by the X-ray diffraction and the selected area electron diffraction patterns. As the Mo content increases, the magnetic hysteresis loops of $Fe_{100-x}Mo_x$ alloy nanowires in parallel to the nanowire axis are not rectangular and the slopes of magnetic hysteresis loops increase. Those results indicate that the magnetostatic interactions between nanowires and the magnetocrystalline anisotropy both have significant influences on the magnetization reversal process of the nanowire arrays.

Keywords: amorphous materials, $Fe_{100-x}Mo_x$, magnetic properties

PACS: 75.50.Kj, 75.50.Bb, 75.30.Gw **DOI:** 10.1088/1674-1056/20/5/057502

1. Introduction

Quasi-one-dimensional magnetic nanowire arrays open up significant opportunities for the ultra-high-density magnetic recording media based on the pattern structure.[1,2] Up to now, nanowire arrays such as metal alloys,[3−5] ferrites[6] and chemical compounds[7,8] have been comprehensively investigated and the magnetization reversal mechanism for guiding practical applications has been explored.[9] In despite of the strong shape anisotropy, for actual nanowire arrays, the magnetocrystalline anisotropy and the magnetostatic interactions between nanowires also have significant influences on the magnetization reversal process.[10] The contributions of the shape anisotropy, the magnetocrystalline anisotropy and the magnetostatic interactions between nanowires are different. Owing to factors such as the difficulty of controlling the orientation of the magnetocrystalline anisotropy in the process of preparation,[11] the possible changes of the saturation magnetization, the distances between nanowires and the diameters and the lengths of the nanowires in nanoscale,[12] it is difficult to quantitatively analyse the specific influences of the shape anisotropy, the magnetocrystalline anisotropy and the magnetostatic interactions between nanowires upon the magnetization reversal process of the nanowires.

For amorphous nanowire arrays, due to the weak magnetocrystalline anisotropy, the shape anisotropy and the magnetostatic interactions between nanowires have effects on the magnetization reversal process.[13] Moreover, because of the high aspect ratios of the nanowires, the shape anisotropy of each nanowire is approximately the same.[14] Thus contributions of the shape anisotropy and the magnetostatic interactions between nanowires on the magnetic reversal process can be distinguished.[13−15] Based on those researches, by synthesizing the crystal nanowire arrays with ordered orientation, in principle we can analyse the influence of the magnetocrystalline anisotropy on the magnetization reversal process.[11] Consequently, studying simultaneously crystals with ordered orientation and amorphous phase can take advantage of quantitative analysis to understand the magnetocrystalline anisotropy influences on the magnetization reversal process.

The crystals of the Fe–Mo alloy can change from crystalline phase to amorphous phase depending on the Mo content.[16] The electrochemical deposition technology may break the narrow ingredient range of

*Project supported by the National Science Fund for Distinguished Young Scholars, China (Grant No. 50925103), the Key Program of the Chinese Ministry of Education (Grant No. 309027), and the Fund for Academic Newcomer of Ph. D. of Lanzhou University, China.

†Corresponding author. E-mail: gaodq08@lzu.edu.cn

© 2011 Chinese Physical Society and IOP Publishing Ltd

the crystal structure with ordered orientation of the traditional Fe–Mo alloy.[17] In the present work, we synthesized the $Fe_{100-x}Mo_x$ alloy nanowire arrays in two phases: crystalline with ordered orientation and amorphous phase. To facilitate the process of determining more exactly the major sources of the magnetic anisotropy and the exploration of the magnetization reversal process, it is necessary to make further research of magnetic properties of the two phases.

2. Experiments

The $Fe_{100-x}Mo_x$ ($13 \leq x \leq 25$) alloy nanowire arrays were prepared by electrodepositing of $Fe^{2+}$and Mo^{2+} with different ionic ratios into anodic aluminum oxide (AAO) templates. The uniform and ordered AAO templates were fabricated by a two-step anodizing process.[18−21] High purity aluminum foil (99.999%) was degreased and annealed at 500 °C for about 2 h in the atmosphere. The foil was then anodized in a 0.3 M oxalic acid solution under a constant direct-current voltage of 40 V for 30 min at 0 °C. Then the oxide film was dissolved in a mixed solution of 0.2 M H_2CrO_4 and 0.4 M H_3PO_4 for 30 min at 60 °C. Finally, the remained aluminum membrane was anodized for 4 h in the same oxalic acid solution at the same conditions again. The electrodeposition of the nanowires was performed by using a standard double electrode bath. The AAO templates were used as the anode and the graphite was used as the cathode. The electrolyte contained $FeSO_4{\cdot}7H_2O$ and $Na_2MoO_4{\cdot}2H_2O$ with different molar ratios. H_3BO_3 was also added as the buffer. The pH value of the electrolyte was adjusted to 4.0 and the alternating current electrochemical depositions were conducted at 8 V and 200 Hz for a duration of 5 min at room temperature.

The morphologies of the AAO templates were obtained by using the field emission scanning electron microscope (FESEM, Hitachi S-4800). The images of the nanowires were obtained by using the transmission electron microscopy (TEM, JEM-2010), where the nanowires were separated from the AAO templates by dissolving the aluminum oxide templates in the mixed solution of 0.2 M H_2CrO_4 and 0.4 M H_3PO_4. The selected area electron diffraction (SAED) and the X-ray diffraction (XRD, X' Pert PRO PHILIPS with Cu K_α radiation) were employed to study the structure of the nanowires. The compositions of the nanowires were analysed by using the inductively coupled plasma-atomic emission spectrometer (ICP, IRIS, ER/S) with an uncertainty about ±0.01. The magnetic properties of the nanowires were characterized by using the vibrating sample magnetometer (VSM, Lakeshore 7304) at room temperature.

3. Results and discussion

The XRD patterns of the $Fe_{100-x}Mo_x$ alloy nanowires with Mo content ranging from 13 to 25 at% are displayed in Fig. 1. Besides the smooth amorphous broad peaks owing to the Al_2O_3 films, there is a sharp diffraction peak corresponding to the α-Fe-like bcc (110) orientation. As the Mo content increases in the nanowire arrays, the sharp peak gradually decreases. It disappears when the Mo content reaches 25 at%, implying that the nanowires may be in amorphous structure. These results demonstrate that with the increase of the Mo content, the $Fe_{100-x}Mo_x$ alloy nanowires gradually change from crystalline phase to amorphous phase. It can be seen that the diffraction peak has shifted towards the left as compared with that of the α-Fe-like bcc (110) orientation and the maximum shift is about 0.4° for the $Fe_{80}Mo_{20}$ nanowires. The peak shift attributes to the increase of the lattice constant of the $Fe_{100-x}Mo_x$ nanowire, as the radius of Mo atom is larger than that of Fe.[22] The changes of the crystal structure have effect on the magnetocrystalline anisotropy of the $Fe_{100-x}Mo_x$ nanowires.

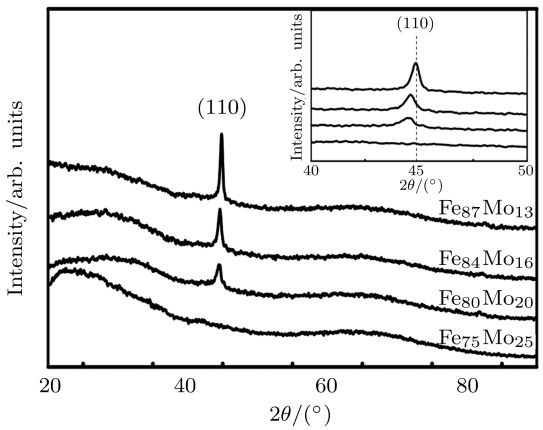


Fig. 1. The X-ray diffraction patterns of AAO templates filled with the $Fe_{100-x}Mo_x$ nanowires of various compositions. The magnified view of the central part of the X-ray diffraction patterns is displayed in the top right inset.

The FESEM image of the AAO template is shown in Fig. 2(a). It is found that the nanopores about 40 nm in diameter are uniform and ordered. The TEM images and the SAED patterns of $Fe_{87}Mo_{13}$ and

$Fe_{75}Mo_{25}$ nanowires are shown in Figs. 2(b) and 2(c), respectively. The TEM results in Figs. 2(b) and 2(c) display that the nanowires are also around 40 nm in diameter with an aspect ratio of about 75, which is consistent with the diameters of the nanopores embedded in the AAO templates. The diffraction result in the SAED pattern shown in Fig. 2(b) demonstrates that the $Fe_{87}Mo_{13}$ nanowires are in crystal structure and the halo in the SAED pattern shown in Fig. 2(c) indicates that the $Fe_{75}Mo_{25}$ nanowires are of the amorphous structures, which are well consistent with the XRD results.

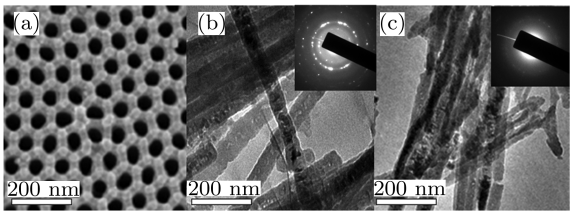


Fig. 2. (a) The FESEM image of the AAO template. (b) The TEM image of the $Fe_{87}Mo_{13}$ nanowires is shown and the top right inset is the corresponding SAED pattern. (c) The TEM image of the $Fe_{75}Mo_{25}$ nanowires is displayed and the top right inset is the corresponding SAED pattern.

Several typical magnetic hysteresis loops of the $Fe_{100-x}Mo_x$ alloy nanowires embedded in the AAO templates measured at room temperature are displayed in Fig. 3, where $\parallel$ and $\perp$ indicate the applied external magnetic field $\boldsymbol{H}$ parallel and perpendicular to the axis of the nanowires, respectively. The different shapes of magnetic hysteresis loops in parallel and perpendicular directions indicate that the nanowires exhibit the uniaxial magnetic anisotropy and the easy magnetization direction is along the axis of the nanowires. We define the slope of the magnetic hysteresis loop as $\tan\theta$, where θ is the angle between the axis of $\boldsymbol{H}$ and the magnetic hysteresis loop. The magnetic hysteresis loops in a parallel direction are not rectangular and the slopes of magnetic hysteresis loops increase with the increase of the Mo content. The infinite cylinder model predicts that the magnetic hysteresis loop of single nanowire should be rectangular with the remanence squareness $M_r/M_s = 1$,[23] where M_r is the remanence magnetization and M_s is the saturation magnetization. When the applied magnetic field is parallel to the axis of the nanowires, the coercivity should equal to the switching field. The magnetic hysteresis loop in parallel to the axis of the nanowires is not rectangular in our experimental results, which may attribute to the influences of the magnetocrystalline anisotropy and the magnetostatic interactions between nanowires.[23] The magnetostatic interactions between nanowires decrease with the increase of the Mo content, because the magnetostatic interactions between nanowires are proportional to the saturation magnetization,[13–15] and the saturation magnetization of the $Fe_{100-x}Mo_x$ alloy nanowire arrays decreases with the increase of the Mo content.[16,24] Besides, according to the XRD results, crystal structures of the $Fe_{100-x}Mo_x$ alloy nanowires change with the increasing Mo content, which leads to the changes of the magnetocrystalline anisotropy. Hence, the magnetostatic interactions between nanowires and the magnetocrystalline anisotropy contribute to the increase of the slopes of magnetic hysteresis loops of the $Fe_{100-x}Mo_x$ alloy nanowire arrays. Those results are in agreement with our experimental results.

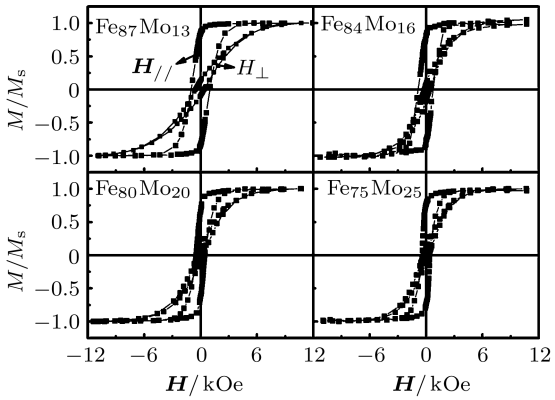


Fig. 3. The magnetic hysteresis loops of AAO templates embedded with the $Fe_{100-x}Mo_x$ nanowires of different contents measured at room temperature (1 Oe = 79.6 $A{\cdot}m^{-1}$).

The $Fe_{75}Mo_{25}$ nanowires are in an amorphous structure. It is well known that the magnetocrystalline anisotropy is very weak in the amorphous structure, therefore the magnetic anisotropy of the nanowires mainly results from the shape anisotropy. The easy magnetization direction is along the axis of the nanowire, because the aspect ratio of the nanowire is high ($\approx$75). In general, the coercivity for the applied magnetic field parallel to the axis of the nanowire is larger than that perpendicular to the axis of the nanowire due to the anisotropy of the geometrical shape of the individual nanowire.

The dependence of the coercivity and the squareness of the magnetic hysteresis loops in parallel to the axis of the nanowires on the composition of the $Fe_{100-x}Mo_x$ nanowires are shown in Fig. 4. It can be seen that with the increase of the Mo

content from 13 to 25 at%, the parallel coercivity $\boldsymbol{H}_{\rm c}(\|)$ decreases from 1016 to 400 Oe (1 Oe = 79.6 A·m^{-1}) and the squareness $M_{\rm r}/M_{\rm s}(\|)$ decreases from 0.86 to 0.64. It is known that the magnetization reversal process has great influence on the coercivity and the squareness. In magnetic nanowires, the magnetization reversal process was explained by the chains-of-spheres model.[25] According to the symmetric fanning, the parallel coercivity $\boldsymbol{H}_{\rm c}(\|)$ of the nanowires is proportional to the saturation magnetization $M_{\rm s}$. The saturation magnetization $M_{\rm s}$ of the $Fe_{100-x}Mo_x$ alloy nanowires decreases with the increase of the Mo content, which is in agreement with the symmetric fanning model.[25]

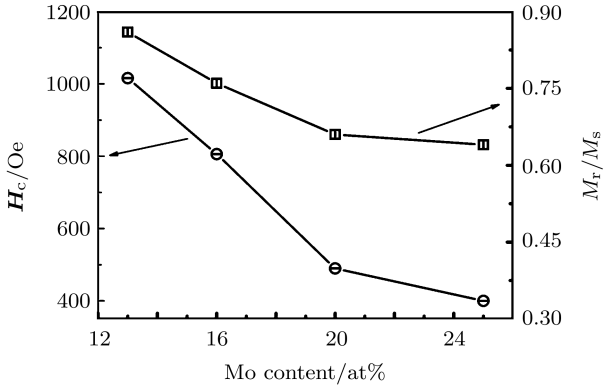


Fig. 4. The dependence of the coercivity and the squareness in parallel to the axis of the nanowires on the composition of the $Fe_{100-x}Mo_x$ (where x is 13, 16, 20 and 25, respectively) nanowires measured at room temperature (1 Oe = 79.6 A·m^{-1}).

4. Conclusions

The $Fe_{100-x}Mo_x$ alloy nanowire arrays with diameters of around 40 nm were fabricated in the AAO templates by the electrochemical deposition method. Structural characterizations show that the nanowires are in the amorphous structure when the Mo content reaches 25 at%. When applying the external magnetic field in the direction of the nanowire axis, the coercivity and the squareness of the nanowires decrease with the increase of the Mo content. The nanowire arrays exhibit the obvious uniaxial magnetic anisotropy with the easy magnetization direction in parallel to the axis of the nanowires owing to the strong shape anisotropy.

References

[1] Chou S Y 1997 *P. IEEE* **85** 652

[2] Bao J C, Tie C Y, Xu Z, Ma Q, Hong J M, Sang H and Sheng D 2002 *Adv. Mater.* **14** 44

[3] Yue G H, Wang L S, Wang X, Chen Y Z and Peng D L 2009 *J. Appl. Phys.* **105** 074312

[4] Almasi Kashi M, Ramazani A, Es'haghi F, Ghanbari S and Esmaeily A S 2010 *Physica* B **405** 2620

[5] Liu L H, Li H T, Fan S H, Gu J J, Li Y P and Sun H Y 2009 *J. Magn. Magn. Mater.* **321** 3511

[6] El-Sheikh S M, Harraz F A and Hessien M M 2010 *Mater. Chem. Phys.* **123** 254

[7] Gao D Q, Fu J L, Xu Y and Xue D S 2008 *Mater. Lett.* **62** 3070

[8] Yuan X Y, Wu G S, Xie T, Lin Y and Zhang L D 2004 *Nanotechnology* **15** 59

[9] Zhan Q F, Gao J H, Liang Y Q, Di N L and Cheng Z H 2005 *Phys. Rev.* B **72** 024428

[10] Henry Y, Ounadjela K, Piraux L, Dubois S, George J M and Duvail J L 2001 *Eur. Phys. J.* B **20** 35

[11] Sánchez-Barriga J, Lucas M, Radu F, Martin E, Multigner M, Marin P, Hernando A and Rivero G 2009 *Phys. Rev.* B **80** 184424

[12] Zeng H, Skomski R, Menon L, Liu Y, Bandyopadhyay S and Sellmyer D J 2002 *Phys. Rev.* B **65** 134426

[13] Prida V M, Vega V, Serantes D, Baldomir D, Ilyn M, Zhukov A P, González J and Hernando B 2009 *Phys. Status Solidi* A **206** 2234

[14] Fodor P S, Tsoi G M and Wenger L E 2003 *J. Appl. Phys.* **93** 7438

[15] Su H L, Ji G B, Tang S L, Chen W, Li Z, Gu B X and Du Y W 2005 *J. Appl. Phys.* **97** 116104

[16] Sumiyama K, Ezawa H and Nakamura Y 1987 *J. Phys. Chem. Solids* **48** 255

[17] Jartych E, Karolus M, Oleszak D, Żurawicz J K, Sarzyński J and Budzyński M 2002 *J. Alloys Compd.* **337** 69

[18] Ren Y, Wang J B, Liu Q F, Han X H and Xue D S 2009 *Chin. Phys.* B **18** 3573

[19] Yang W, Cui C X, Sun J B and Wang B L 2010 *J. Mater. Sci.* **45** 1523

[20] Gao T R, Chen Z Y, Peng Y and Li F S 2002 *Chin. Phys.* **11** 1307

[21] Shi H G, Fu J L and Xue D S 2005 *Acta Phys. Sin.* **54** 3862

[22] Jiraskova Y, Zabransky K, Turek I, Bursik J and Jancik D 2009 *J. Alloys Compd.* **477** 55

[23] Ross C A, Hwang M, Shima M, Cheng J Y, Farhoud M, Savas T A, Smith H I, Schwarzacher W, Ross F M, Redjdal M and Humphrey F B 2002 *Phys. Rev.* B **65** 144417

[24] Aldred A T 1968 *J. Phys.* C: *Solid State Phys.* **1** 244

[25] Zhan Q F, Chen Z Y, Xue D S and Li F S 2002 *Phys. Rev.* B **66** 134436